Propagation velocity and reflection of pressure waves in the canine coronary artery

Propagation velocity and reflection of pressure waves in the canine coronary artery

T. ARTS, R. T. I. KRUGER, W. VAN GERVEN, J. A. C. LAMBREGTS, AND R. S. RENEMAN
Departments of Biophysics and Physiology, University of Limburg, Maastricht 6200 MD, The Netherlands; and Cardiovascular Department, Janssen Pharmaceutica, Beerse, Belgium

ARTS, T., R. T. I. KRUGER, W. VAN GERVEN, J. A. C. LAMBREGTS, AND R. S. RENEMAN. *Propagation velocity and reflection of pressure waves in the canine coronary artery.* Am. J. Physiol. 237(4): H469–H474, 1979 or Am. J. Physiol.: Heart Circ. Physiol. 6(4): H469–H474, 1979.—In this study the pressure wave velocity in the anterior descending branch of the left coronary artery (LADC) of the dog was measured by determining the delay time between pressure pulses along this artery. This method can only be applied if reflections of the pressure wave distal to the sites of pressure measurement are insignificant. From araldite casts of the coronary arteries the following relation between the diameter proximal to (d_{prox}) and distal to ($d_{dist\,1}$, $d_{dist\,2}$) a bifurcation was found: $d_{prox}^{2.55} = d_{dist\,1}^{2.55} + d_{dist\,2}^{2.55}$, indicating that reflections at a bifurcation are minimal. In dogs reflections were studied by inducing during diastole a pressure pulse in the aorta and measuring pressure and volume flow proximal to and pressure distal to a segment of the LADC at various levels of the coronary peripheral resistance. Reflection of high-frequency components (>7 Hz) was found to be insignificant, allowing application of the above-mentioned method for measuring the wave-front velocity, which is insensitive to low-frequency reflection. At a pressure in the LADC of 13.3 kPa this velocity was 8.6 ± 1.4 $m \cdot s^{-1}$ (mean ± SD). The calculated dynamic cross-sectional stiffness ($\Delta P/(\Delta A/A)$) of the LADC was 97 ± 11 kPa (mean ± SE) at an arterial pressure of 13.3 kPa.

epicardial coronary arteries; coronary casts; coronary bifurcations; coronary peripheral resistance; dynamic cross-sectional stiffness

IN DESCRIBING THE PHYSICAL PROPERTIES of the coronary arteries, their dynamic capacitance, defined as the ratio of the increment in volume to the increment in pressure for a fast pressure change, is an important quantity. This capacitance has been determined in vitro and appeared to be smaller than the static capacitance (2, 5, 6). However, the results obtained in those studies are not necessarily representative of the in vivo situation. The dynamic capacitance in vivo is related to the velocity of a pressure wave front in the arteries investigated. This velocity has been determined in several arteries (3, 9, 10, 11) but, to our knowledge, not in the epicardial coronary arteries.

In the present study the pressure wave velocity in diastole was determined in vivo in a segment of the anterior descending branch of the left coronary artery (LADC). A pressure-pulse wave was generated in the abdominal aorta, and its velocity in the LADC was determined by measuring the delay time between the pressure pulses recorded proximal and distal to the segment of the LADC. This method, however, can only be used, if reflections of the pressure wave distal to the sites of pressure measurement are insignificant. Therefore, the magnitude of these reflections has to be known. Possible sources of reflections in the coronary vasculature are bifurcations and the coronary peripheral resistance.

Information about reflections at bifurcations was obtained from the relation between artery diameters proximal and distal to bifurcations, as determined in araldite casts of the coronary vasculature. Reflections at the peripheral resistance were studied in in vivo experiments by analyzing proximally in the vessel under investigation the changes in pressure and volume flow induced by a pressure pulse, generated during diastole at various levels of this resistance.

METHODS

In vitro experiments (casts). The experiments were performed on nine mongrel dogs of varying weight, unknown age, and of either sex. Under anesthesia the animals were killed by bleeding, and the hearts were removed and weighed. The coronary arteries were cast with araldite (F type HY943) at a filling pressure of 13.3 kPa in four hearts and 25.3 kPa in five other hearts.

Each cast of the coronary arteries was divided into three trees, corresponding to the perfusion areas of the right coronary artery (RC), the anterior descending branch (LADC), and the circumflex branch (LCC) of the left coronary artery, respectively. The septal branch was arbitrarily considered to be part of the LADC. All branches smaller than 0.4 mm in diameter were removed. The diameter of the remaining branches was measured in relation to their position with a vernier caliper.

The magnitude of the reflections at a bifurcation depends on the relation between the diameters of the branches proximal and distal to that bifurcation. This relation was studied in 12 trees of the coronary casts (4 LADC, 4 LCC, and 4 RC). In each tree for all branches larger in diameter than 0.4 mm the number N of distal branches with a diameter of 0.4 mm was determined. The branches were grouped according to their diameter, starting at a diameter of 0.5 mm and increasing in steps of 0.1 mm up to the largest branch diameter of the tree.

0363-6135/79/0000-0000$01.25

The average of N in each diameter group ($\bar{N}$) was plotted as a function of that branch diameter. The best fitting regression was calculated.

To evaluate the accuracy of the diameter measurements in the casts, the length of the branches was measured as well. The volume of 16 trees (6 LADC, 5 LCC, and 5 RC), as calculated from the length and diameter measurements, was compared with the volume of these trees measured directly by determination of the buoyant force caused by the volume displacement of the tree submerged in water.

In vivo experiments. The experiments were performed on 10 mongrel dogs of either sex, unknown age, and ranging in weight from 28 to 45 kg. The animals were premedicated with a combination of fluanisone (10 mg/kg body wt) and Fentanyl base (0.2 mg/kg body wt) as described by Marsboom et al. (7). Anesthesia was induced with sodium pentobarbital (10 mg/kg body wt iv) and after endotracheal intubation, was maintained by oxygen-nitrous oxide. Ventilation was kept constant during the experiment with a positive-pressure respirator (Bird).

The experimental setup is schematically shown in Fig. 1. The ECG was derived from the limb leads. Ascending aortic pressure was measured through the left carotid artery with a polyethylene catheter connected to a pressure transducer (Telco RA9). The chest was opened through the left fifth intercostal space, and the heart was suspended in a pericardial cradle. Coronary artery pressure was measured in the first two major side branches of the LADC with short (25 mm) stainless steel needles (ID 0.95 mm). The blunt tip of each needle was positioned at the origin of the branch by palpation. Millar (PC-470) catheter-tip micromanometers were plugged into the connector cones of both needles. This system had a rather high frequency response (100 Hz, −3 dB) and artifacts due to movements of the catheter were absent. To avoid clotting, heparin (200 U/kg body wt) was administered intravenously. After each hour an additional dose of 100 U/kg body wt was given. An electromagnetic flow probe was placed on the LADC proximal to the sites of pressure measurement and was connected to a sine wave electromagnetic flowmeter (Transflow 600) with an upper frequency response of 100 Hz (−3 dB). The flow probe was calibrated in vivo as described previously (13).

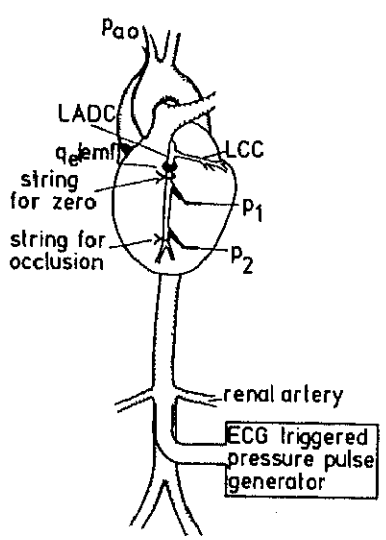

FIG. 1. Experimental set-up for the in vivo measurements; P_1 and P_2 are the sites of pressure measurement proximal and distal to the segment of the LADC; q_e is flow in the LADC as determined electromagnetically; P_{ao} is aortic pressure.

The determined variables were recorded on a Schwarzer 10-channel physiological recorder (frequency response: 150 Hz, −3 dB; speed 200 mm/s) and on a Hewlett-Packard (3521B) electromagnetic tape recorder (speed 15 inch/s). The pressure pulses were also displayed on an oscilloscope (Tektronix, type R5031).

An ECG-triggered pressure-pulse generator (Dreyssen) was connected to the abdominal aorta through a PVC tube with an inner diameter of 9 mm. The tube was placed in the aorta approximately halfway between the renal arteries and the iliac bifurcation. An adequate pressure pulse with a rise time of 10 ms could be generated by rapid injection of 20 ml of blood into the abdominal aorta. Shorter rise times could not be achieved. Moreover, pressure signals with a rise time shorter than 10 ms contain important frequency components over 30 Hz. At these high frequencies the elastic properties of the artery might be changed, resulting in errors in the determination of the pressure wave velocity. The distance between the sites of pressure measurement, being the distance between the first large side branches of the LADC, was generally 20–30 mm.

After installation of the measuring devices and the pressure generator, the latter was filled with 200 ml of blood from the aorta by slow suction. The delay between the ECG and the pump was adjusted so that the pressure pulse arrived in the coronary system approximately 100 ms after closure of the aortic valve (Fig. 2). The wavefront velocity (v_{wf}) in the LADC was defined as the ratio of the distance between the sites of pressure measurement to the time interval (Δt) between the change in pressure at the proximal and distal sites of measurement. The signals were compared at 25% of the maximum pressure change (Fig. 3*A*). At levels higher than 25% of the maximum pressure change, irregularities in the rising slope of the pressure signal were more pronounced. These irregularities probably resulted in part from reflection of the pressure wave in the aorta at the aortic valve.

Under control conditions several series of approximately 10 pulses were generated while the variables were recorded continuously. After each series of pulses the pump was refilled with blood. After the control series a coronary vasodilator, dipyridamole (5 mg/kg body wt), was administered intravenously. When the flow in the LADC had reached a higher stationary level, a similar series of pulses was generated as in the control situation. To induce reflections the LADC was temporarily occluded distal to the sites of pressure measurement and several series of pulses were generated.

RESULTS

In vitro experiments. The average number of distal branches ($\bar{N}$) 0.4 mm in diameter belonging to one branch was determined as a function of the diameter (d) of that branch. Figure 4 shows the experimental data for 12

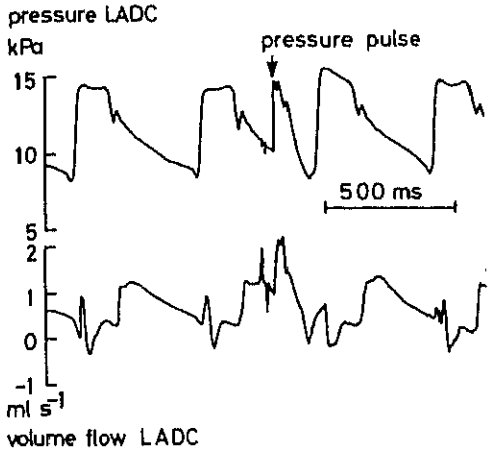

FIG. 2. Pressure (P_1) and volume flow curves proximally in the LADC. The recorded pressure pulse arrived approximately 100 ms after closure of the aortic valve. The rising slope of this pressure pulse is shown in more detail in Fig. 3*A*.

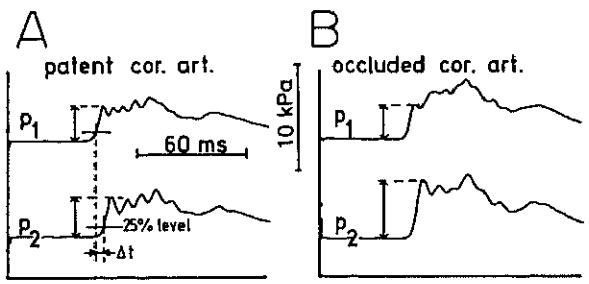

FIG. 3. Pressure pulse as recorded proximal (P_1) and distal (P_2) to a segment of the LADC, both before (*A*) and after (*B*) occlusion of the LADC distal to P_2. Δt represents the delay between the 25% levels (*small horizontal lines*) of the pressure pulse. These registrations are made during diastole. The rising slope of the pulses starts approximately 100 ms after closure of the aortic valve.

trees. From 183 data points the following relation between $\bar{N}$ and d (correlation coefficient 0.988) was found

$$\bar{N}(d) = (d/d_0)^s \qquad (1)$$

with $d_0 = 0.38 \pm 0.01$ mm (mean ± SE) and $s = 2.55 \pm 0.03$ (mean ± SE).

A relation between the vessel diameters proximal and distal to a bifurcation was derived from this equation. Suppose that at a branch point, branch "prox" bifurcates into branch "dist 1" and "dist 2," and the number of distal branches of 0.4 mm, belonging to these branches are N_{prox}, $N_{dist\,1}$, and $N_{dist\,2}$, respectively. Obviously it holds that

$$N_{prox} = N_{dist\,1} + N_{dist\,2} \qquad (2)$$

Substitution of the experimental *relation 1* into *relation 2* renders

$$d^s_{prox} = d^s_{dist\,1} + d^s_{dist\,2} \qquad (3)$$

After substituting $s = 2.55$ this relation implies for a symmetric bifurcation ($d_{dist\,1} = d_{dist\,2}$) a ratio of the proximal to distal branch diameters of 1.31, which agrees perfectly with the theoretical value for minimum reflection at a bifurcation which is also 1.31 (APPENDIX).

The accuracy of the length and diameter measurements in the casts is indicated by the excellent agreement between the volumes computed from these dimensions and the volumes measured directly. In measurements on 16 trees it was found that the ratio of calculated to measured volume was 1.003 ± 0.012 (mean ± SE).

In vivo experiments. In a patent coronary artery (Fig. 3*A*) proximal and distal to a segment of the LADC the recorded pressure pulses were similar. After occlusion of the LADC distal to the sites of pressure measurement (Fig. 3*B*), the ascending part of the distal pressure pulse increased to approximately twice its original value. This increase indicates that total reflection of the high-frequency components of the pressure signal occurs under these circumstances. Reflection of low-frequency components could not be detected because the distances in the coronary system are short compared to the related wavelength. The similarity of the pressure pulses recorded proximally and distally in the patent LADC (Fig. 3*A*) indicates that high-frequency reflections are insignificant under these circumstances.

From the theory on wave propagation and reflections in transmission lines (7) it follows that a wave is not reflected if the input impedance at the entrance of the LADC is equal to the characteristic impedance of that vessel. This characteristic impedance is determined by the physical properties of the LADC and, therefore, is independent of the coronary peripheral resistance. To study reflection of low-frequency components the effect of changes in coronary peripheral resistance on the input impedance of the LADC was investigated. For this purpose pressure pulses were generated in the aorta at different levels of the coronary peripheral resistance. Changes in the input impedance of the LADC were detected from the responses of pressure and volume flow

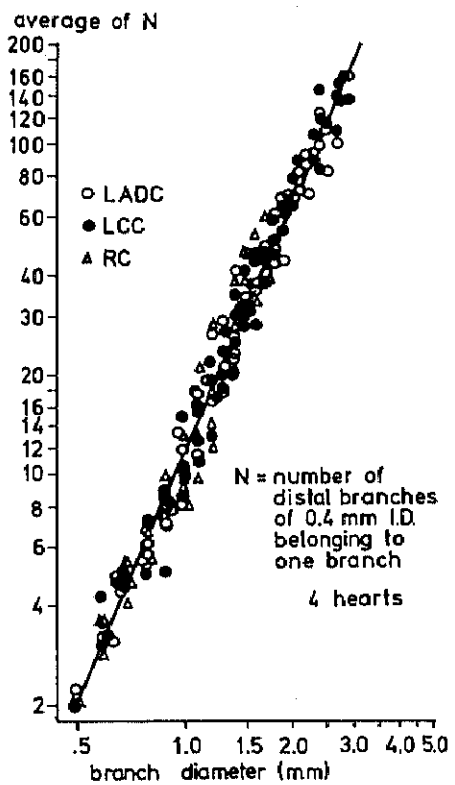

FIG. 4. Average number of branches 0.4 mm in diameter distal to a coronary artery branch as a function of the diameter of that branch.

proximally in the LADC to these pressure pulses.

The solid tracings in Fig. 5 are pressure and volume flow recorded proximally in the LADC during part of diastole following the induction of a pressure pulse in the abdominal aorta in the control situation. The dotted lines in Fig. 5 represent the pressure and volume flow tracings when the aortic pressure pulse was generated at a coronary peripheral resistance reduced to approximately half the normal value by administration of dipyridamole. Despite the similarity of the pressure tracings, the recordings of coronary artery volume flow appear to be different. This difference implies a change of the input impedance of the LADC induced by a change in peripheral resistance and, hence, the existence of reflections. The ascending part of the volume flow tracing is approximately the same in both situations, which indicates that reflections at high frequencies (>7 Hz) are not affected by changes in peripheral resistance. This finding agrees with the previous finding that at high frequencies hardly any reflections were detected. Fourier analysis of the difference between both volume flow recordings reveals that components in the signal below 7 Hz are reflected significantly by the coronary peripheral resistance.

The wave-front velocity. Since the wave-front velocity is a function of arterial blood pressure, this velocity was determined at 25% of the maximum pressure change, following the induction of the pressure step in the abdominal aorta. In each dog the data on the wave-front velocity were grouped according to the various pressure levels, so that for some dogs more than one velocity value was obtained. The mean wave-front velocities at a certain pressure level and the corresponding 95% reliability intervals were computed. The results are shown in Fig. 6. At lower pressure levels the reliability interval is smaller and the density of measurements is higher. Therefore, a fit with a logarithmic curve was made. The following relation between wave-front velocity (v_{wf}) and coronary artery pressure (P) was found with a correlation coefficient of 0.86

$$v_{wf} = 1.44\ P^{0.69}$$

where v_{wf} is expressed in $m \cdot s^{-1}$ and P in kPa. At a coronary artery pressure of 13.3 kPa (100 mmHg) the wave-front velocity was found to be

$$v_{wf} = 8.6 \pm 1.4\ m \cdot s^{-1}\ (\text{mean} \pm \text{SD})$$

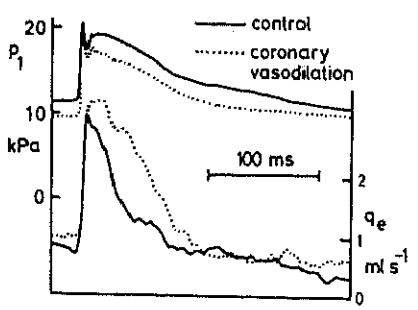

FIG. 5. Pressure (P_1) and volume flow (q_e) as recorded proximally in the LADC during diastole following the induction of a pressure pulse in the abdominal aorta at normal (*solid line*) and reduced (*dotted line*) coronary peripheral resistance. The rising slope of the pressure pulses starts approximately 100 ms after closure of the aortic valve.

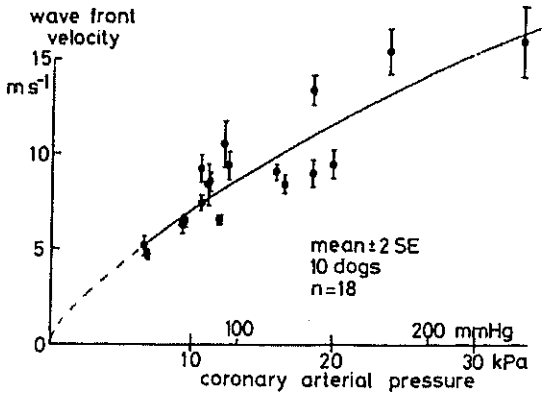

FIG. 6. Wave-front velocity as a function of coronary artery blood pressure, determined at 25% of the maximum pressure change following induction of a pressure pulse in the abdominal aorta.

DISCUSSION

In the present study the wave-front velocity in coronary arteries during diastole was determined in the in vivo situation. The method to determine the wave-front velocity from the delay between pressure signals recorded along the artery is only valid if reflections are absent or low in amplitude. The cast experiments indicated that coronary artery branches were ideally matched so that the reflection of pressure waves at bifurcations was likely to be minimal. From the in vivo studies it could be concluded that frequencies below 7 Hz were reflected at the coronary peripheral resistance. Above 7 Hz the amplitude of reflections was not influenced by changes in the coronary peripheral resistance. At these high frequencies reflections were apparently small in amplitude. This was supported by the finding that the shapes of the pressure tracings proximal and distal to the segment of the LADC were similar when a pressure pulse was generated in the abdominal aorta. The method for determining the wave-front velocity used in this study seems reliable because the method is rather insensitive to low-frequency components (<7 Hz) in the pressure signals. The components of the pressure signal, which represent the rising slope of the pressure pulse, contain predominantly high-frequency components (up to 30 Hz). At an arterial pressure of 13.3 kPa the average value of the wave-front velocity in the LADC as found in this study (8.6 $m \cdot s^{-1}$) appeared to be significantly lower than the wave-front velocity in the tibial artery (12 $m \cdot s^{-1}$) as reported by McDonald (9). This finding suggests that coronary arteries are more compliant than systemic arteries of similar size, which was also reported by Douglas et al. (5).

One may wonder whether the relation of the diameter proximal and distal to a bifurcation found in the casts can be extrapolated to the in vivo situation. During the casting procedure diameter changes may occur due to variations in arterial pressure and mechanical properties of the arterial wall at various sites in the coronary vasculature. The pressure during casting is likely to be similar in all coronary artery branches because araldite flow is viscous prior to hardening. This viscous flow behavior implies maximum flow resistance in the far distal parts of the arterial vasculature (at the level of arterioles), whereas the pressure drop in the proximal

epicardial vessels is negligible. Changes in mechanical properties of the arterial wall during the process of casting are likely to be the same for all coronary arteries with an internal diameter larger than 0.4 mm. This is indicated by the finding that the ratio of wall thickness to vessel radius is constant for all coronary artery branches with a diameter larger than 0.3 mm (4). Because of the uniformity of the casting pressure and the similar mechanical properties of the arterial wall at various sites in the coronary vasculature, the ratio of the diameters proximal and distal to a bifurcation is probably not affected by the casting procedure. Therefore, extrapolation of the findings in the casts to the in vivo situation should be allowed.

The results obtained in this study indicate that the velocity of a pressure wave in the epicardial coronary arteries can be assessed in vivo. Application of theories on pressure wave propagation in arteries (3, 10, 14) to these results gives the dynamic cross-sectional stiffness K, defined as the ratio of pressure increment to the relative increment in cross-sectional area ($\Delta A/A$). The value of K, calculated on the basis of the present findings, is 97 ± 11 kPa (mean ± SE) at an arterial pressure of 13.3 kPa (100 mmHg). Douglas et al. (5) as well as Gow et al. (6) deduced a stiffer behavior of the epicardial coronary arteries (K = 176 + 29 kPa, mean ± SE, and K = 205 kPa, respectively, at an arterial pressure level of 13.3 kPa). The differences between their results and ours could be explained by different experimental setups. In the studies of Douglas et al. and Gow et al., after all, the dynamic stiffness of the epicardial coronary arteries was determined in vitro.

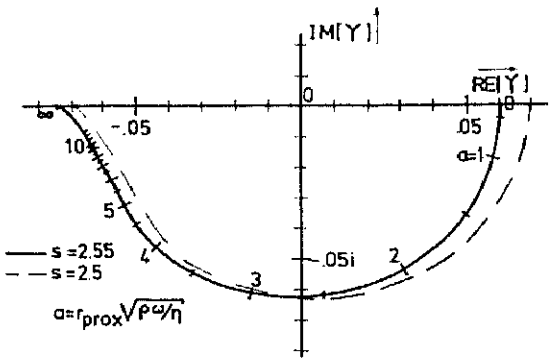

FIG. 7. Reflection coefficient (γ) at a bifurcation of a coronary artery in the complex plane as a function of $r_{prox}\sqrt{\rho\omega/\eta}$, where r_{prox} = radius of the proximal branch; ρ = density of blood, ω = angular frequency, and η = viscosity of blood.

APPENDIX

Computation of the Reflection Coefficient at a Symmetrical Bifurcation

From *relation 3* for the internal radius in a symmetric bifurcation it can be derived that

$$r_{prox}/r_{dist} = 2^{1/s} \tag{4}$$

where r_{prox} and r_{dist} are the radii of the proximal and two distal branches, respectively. In the analysis, reflection is considered to be a result of unmatched characteristic impedances of the branches at a bifurcation. For a sine wave the characteristic impedance of a branch with radius r equals

$$Z_{0\,prox} = \frac{1}{\pi r^2}\sqrt{\rho K/F(a)} \tag{5}$$

where $a = r\sqrt{\rho\omega/\eta}$ (according to Womersley (14)); and $F(a) = J_2(a\sqrt{-i})/J_0(a\sqrt{-i})$, where i is the imaginary unit, J_0, J_2 are Bessel functions (1), ω = angular frequency, η = viscosity of blood, ρ = density of blood, and $K = \Delta P/(\Delta A/A)$, with ΔP = internal pressure increment, A = cross-sectional area of the vessel, and ΔA = increment of A.

The reflection coefficient at the bifurcation is

$$\gamma = (Z - Z_{0\,prox})/(Z + Z_{0\,prox}) \tag{6}$$

where Z represents the distal loading impedance of the proximal branch, being the two distal characteristic impedances in parallel

$$Z = Z_{0\,dist}/2 \tag{7}$$

When assuming an equal K value for all branches, substitution of *4*, *5*, and *7* into *6* results in

$$\gamma = (q-1)/(q+1) \text{ with } q = 2^{-(1+2/s)}\sqrt{F(a_{prox})/F(a_{prox}\times 2^{-1/s})} \tag{8}$$

In Fig. 7 the solid line shows the pathway of the reflection coefficient in the complex plane with s = 2.55 (r_{prox}/r_{dist} = 1.31) according to *relation 8*. The distance from the origin represents the magnitude of the reflection coefficient and the angle between the positive real axis (RE [γ]), and a point on the curve represents the phase angle of the reflection coefficient. The curve is close to a circle around the origin, which implies that the amplitude of the reflection coefficient is nearly constant (≃6%) in a wide range of frequencies. The sensitivity of the reflection coefficient to variations in s is indicated by the dashed line (Fig. 7) representing the pathway for s = 2.5 (r_{prox}/r_{dist} = 1.32). Then the circle is shifted, resulting in higher values for the reflection coefficient (≃7%) at low frequencies. Obviously, the experimentally determined value of s = 2.55 is very close to the optimal value for minimum reflection in a wide frequency range.

The authors are greatly indebted to Mrs. R. Borgman for her help in preparing the manuscript and to Prof. Dr. P. C. Veenstra and Dr. J. Spaan for their stimulating discussion. The technical assistance of Mr. A. van Glabbeek in preparing the araldite casts is gratefully acknowledged.

This work was supported by the Foundation for Medical Research FUNGO, which is subsidized by the Netherlands Organization for the Advancement of Pure Research.

Received 11 January 1979; accepted in final form 20 June 1979.

REFERENCES

1. ABRAMOWITZ, M., AND I. A. STEGUN. *Handbook of Mathematical Functions* (9th ed.). New York: Dover 1970, p. 692.
2. BERGEL, D. H. The dynamic elastic properties of the arterial wall. *J. Physiol. London* 156: 458–469, 1961.
3. Cox, R. H. Determination of the true phase velocity of arterial pressure waves in vivo. *Circ. Res.* 29: 407–418, 1971.
4. DEBRABANDER, M., AND W. SCHAPER. Quantitative histology of the canine coronary collateral circulation in localized myocardial ischemia. *Life Sci.* 10: 857–868, 1971.
5. DOUGLAS, J. E., AND J. C. GREENFIELD. Epicardial coronary artery compliance in the dog. *Circ. Res.* 27: 921–929, 1970.
6. GOW, B. S., D. SCHONFELD, AND D. J. PATEL. The dynamic elastic properties of the canine left circumflex artery. *J. Biomech.* 7: 389–395, 1974.
7. GRAY, D. E. *American Institute of Physics Handbook* (3rd ed.). New York: McGraw, 1972, part 5, p. 59.
8. MARSBOOM, R. A., D. VERSTRAETE, D. THIENPONT, AND D. MATTEEUWS. The use of haloanisone and phentanyl for neuroleptanalgesia in dogs. *Br. Vet. J.* 120: 466–468, 1964.
9. MCDONALD, D. A. Regional pulse-wave velocity in the arterial tree. *J. Appl. Physiol.* 24: 73–78, 1968.
10. MCDONALD, D. A. *Bloodflow in Arteries.* Southampton: Camelot, 1974, p. 283–308, and 418.
11. O'ROURKE, M. F. Pressure and flow waves in systemic arteries and

anatomical design of the arterial system. *J. Appl. Physiol.* 23: 139–149, 1967.
12. PATEL, D. J. AND J. JANICKI. Static elastic properties of the left circumflex artery and common carotid artery in dogs. *Circ. Res.* 27: 149–158, 1970.
13. RENEMAN, R. S., H. F. CLARKE, N. SIMMONS, AND M. P. SPENCER. In vivo comparison of electromagnetic and Doppler flow meters with special attention to the processing of an analog Doppler flow signal. *Cardiovasc. Res.* 7: 557–566, 1973.
14. WOMERSLEY, J. R. Method for the calculation of the velocity, rate of flow and viscous drag in arteries when the pressure gradient is known. *J. Physiol. London* 127: 553–563, 1955.